Diagnosis of Induction Machines' Rotor Faults in Time-Varying Conditions

Andrea Stefani, Alberto Bellini, *Member, IEEE*, and Fiorenzo Filippetti, *Member, IEEE*

***Abstract*—Motor current signature analysis is the reference method for the diagnosis of induction machines' rotor faults; however, in time-varying conditions, it fails as slip and speed vary, and, thus, sideband components are spread in a bandwidth that is proportional to the variation. Variable speed drive applications are common in the aerospace, appliance, railway, and automotive industries and also in electric generators for wind turbines. In this paper, a simple and effective method is presented that allows the diagnosis of rotor faults for induction machine drives in time-varying conditions. It is tailored to direct rotor flux field-oriented controlled drives, where the control system provides suitable signals that are exploited for the demodulation to a constant frequency of time-varying signatures related to the rotor faults. Simulations and experiments are reported to validate the proposed method on a critical speed transient.**

***Index Terms*—Fault diagnosis, induction motor drives, time-varying systems.**

I. Introduction

INDUCTION motors are widely used in industrial applications for their intrinsic ruggedness and reduced cost. Recently, the use of adjustable speed drives has spread in many applications. Online diagnosis and the early detection of faults in induction machines have focused the attention of researchers since they allow the reduction of maintenance costs and downtime.

In some applications, where continuous operation is a key item, such as railway applications and wind generators, the need for a preventive fault diagnosis is an extremely important point. As an example, the case of railway applications is investigated in [1] and [2] to design a traction drive oriented to maximum fault tolerance. In [3], the use of the Vienna monitoring method (VMM) is investigated for a traction drive application, where rotor fault detection was successfully verified in transient and steady-state conditions.

In this paper, fault detection and the prognosis of rotor faults are critical for industrial applications, although rotor faults share only about 20% of the overall induction machine faults [4]. In fact, the breakage of a bar leads to high current in adjacent bars, thus leading to potential further breakage and stator faults as well.

Manuscript received March 1, 2008; revised February 18, 2009. First published March 16, 2009; current version published October 9, 2009.

A. Stefani and F. Filippetti are with the Department of Electrical Engineering, University of Bologna, 40136 Bologna, Italy.

A. Bellini is with the Department of Engineering Sciences and Methods, University of Modena and Reggio Emilia, 42100 Reggio Emilia, Italy (e-mail: alberto.bellini@unimore.it).

Color versions of one or more of the figures in this paper are available online at http://ieeexplore.ieee.org.

Digital Object Identifier 10.1109/TIE.2009.2016517

Motor current signature analysis (MCSA) was extensively used to detect broken rotor bars and end-ring faults in induction motors [5]–[8]. In steady-state conditions, a quite robust diagnostic index is the sum of the amplitudes of the left and right sideband components of the stator current that is independent of inertia and proportional to the number of adjacent broken bars. The main shortcoming of the MCSA is its dependence on machine slip s, speed, and load, although the dependence on the load torque variations can be compensated for [9]. Moreover, the MCSA fails for current-controlled drives, as the control loop masks the oscillation of the stator current. If an ideal control loop is considered, the controlled variable is desensitized, and anomalous lines appear in the manipulated variables. In actual conditions, depending on the bandwidth, either the manipulated (voltage) or the controlled (current) variable spectrum is more sensitive to the fault. Hence, new diagnostic indexes can be used that are based on control variables [10]–[12].

Other techniques have been investigated for rotor faults beyond the MCSA or its variants. Several demodulation methods were presented to extract fault information from the current. In [13], envelope analysis, Hilbert transformation, and Park transformation were used to perform amplitude demodulation of rotor faults. Other methods were based on multiple electrical signals such as torque and leakage flux. The VMM [14] relies on voltage, current signals, and measured rotor position to check deviations in terms of instantaneous torque obtained by two different machine models. Also, signal injection techniques were proposed, relying on methods that are similar to those adopted for sensorless drive control [15].

Anyway, for time-varying conditions, the most commonly adopted techniques are based on time–frequency analysis. Complex techniques were presented to cope with this issue, including high-frequency resolution methods [16], time–frequency distributions [17], [18], and wavelets [19]–[22]. All the above methods require heavy computation and complex procedures to analyze the time–frequency distribution and to retrieve the information related to rotor faults. Although the computation time itself is not an issue provided that data are sampled, stored, and postprocessed, in industrial applications, the requirement of minimum complexity is a mandatory issue. In fact, with time–frequency analysis, a few major shortcomings appear.

1) The latency is very high, and a large memory is required to store the data that will be processed.
2) A large number of samples are required to achieve reliable results.
3) Specialized hardware is required.

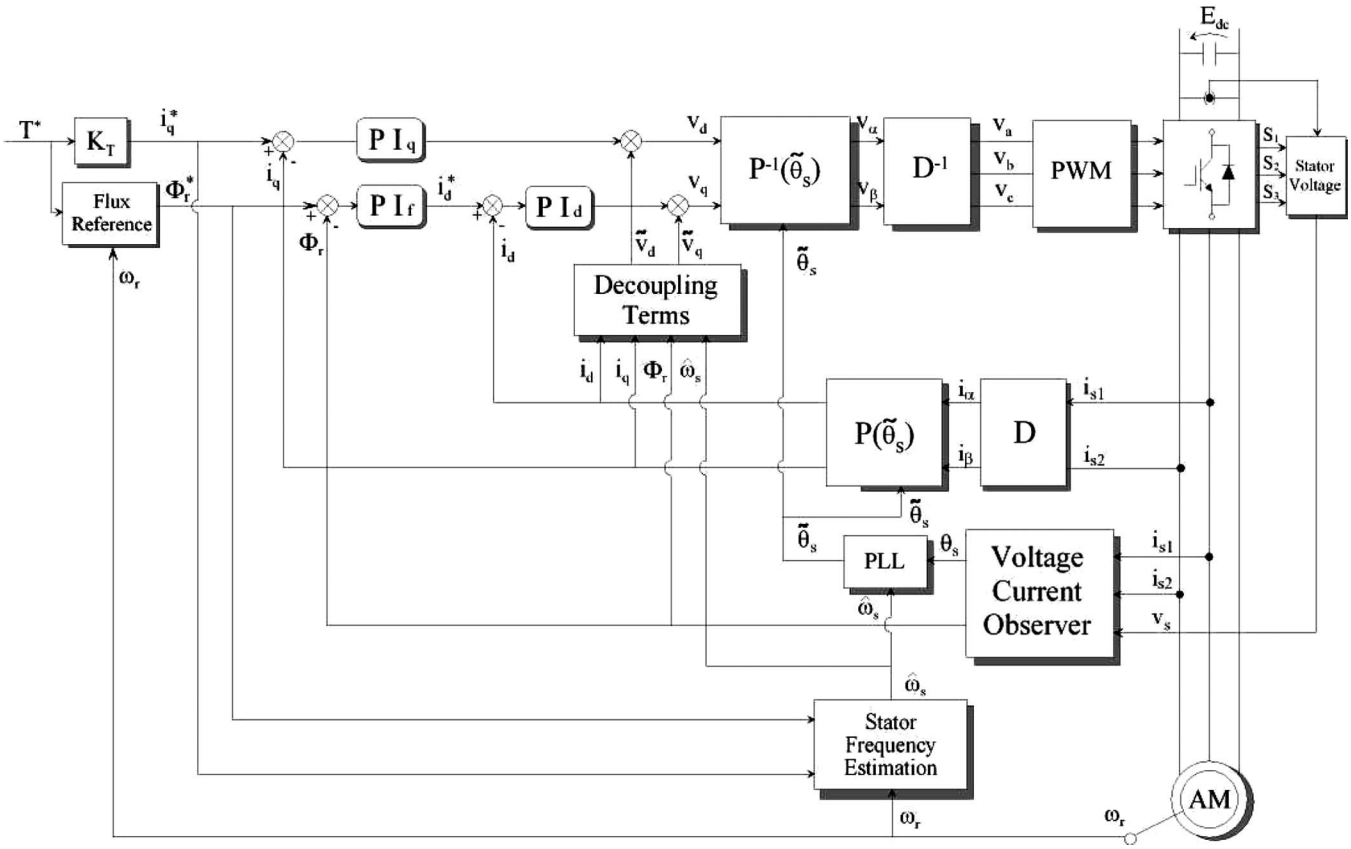

Fig. 1. Block diagram of the control scheme for a typical direct rotor flux field-oriented vector drive.

A simpler method could provide accurate fault detection in time-varying conditions even with a reduced number of samples. Moreover, it can be included in the available firmware used for the drive control, allowing the realization of an effective fault diagnosis at no additional hardware cost.

A typical example of transient behavior is the case of traction applications, where torque and speed vary depending on the journey, preventing the use of the MCSA and classical spectral analysis. In this paper, experiments are performed referring to the typical specifications of a railway application system; however, the proposed method is general, provided that a similar control architecture is used in the drive.

Electric drives for traction applications operate in a field-weakening mode at the cruise speed. Nevertheless, the most relevant accelerations are usually in the constant torque mode since the load torque is lower, being proportional to the square of the speed. Here, reference is made to time-varying conditions and, thus, to constant torque mode.

The issue of rotor fault detection can be solved if a diagnostic index is defined that is independent of slip and stator frequency. Here, a simple demodulation procedure in the time domain is proposed that processes the stator currents, relying on stator frequency and machine slip accurately retrieved by the drive control. After the demodulation process, a component is obtained, whose amplitude is related to the rotor fault and whose frequency is constant, independently of the stator frequency and speed.

This paper is organized as follows. Section II describes a typical induction machine drive for high-power applications. Section III describes the demodulation technique to compute a component that is independent of slip and stator frequency, a diagnostic index that is suitable for time-varying conditions, and the proposed diagnostic procedure. Section IV reports the simulation results to validate the proposed method, and Section V reports the experimental results for an induction machine drive. The results obtained with the proposed approach are compared with the classical spectral analysis methods to demonstrate their performance.

The demodulation technique presented here is applied to stator currents but can also be applied to other variables to extract the faulty components.

II. Control Strategy of Induction Machine Drives

Nowadays, common solutions for high-power applications are based on drives that include a voltage source inverter (VSI) feeding an induction motor or a permanent magnet synchronous motor. However, old-fashioned solutions based on a current source inverter or on thyristors are still employed, whereas old schemes based on dc series motors or direct dc motors are no longer used. Different control schemes are adopted and tailored to the specific application. Typically, variable structure controls are used for high-performance traction drive systems that change according to the operating conditions, particularly according to the speed and flux levels. The basic structure is a direct rotor flux field-oriented vector control, whose scheme is shown in Fig. 1. The vector control algorithm consists of two current loops for flux and torque regulation. Moreover, an

external rotor flux loop is used to set the flux level by means of the direct stator reference current. A similar control structure is used in high-power applications, where transient operations often occur.

Direct and inverse Clark transformations are represented by blocks D and D^{-1}, respectively. Standard PI regulators with antiwindup systems are used for the control loops in a dq reference frame that is synchronous with the rotor flux. The rotor flux is estimated through a stator-model-based observer obtained by integrating the stator voltage equation and taking into account the leakage flux [23] as

$$\overline{\phi}_r = \frac{L_m}{L_r}\left[\int(\overline{v}_s - R_s\overline{i}_s)dt - \sigma L_s\overline{i}_s\right] \tag{1}$$

where L_m is the magnetizing inductance, L_r is the rotor inductance, and L_s is the stator inductance. $\overline{v}_s$ and $\overline{i}_s$ are the space vectors of the stator voltage and current, respectively; $\sigma = 1 - L_m^2/L_sL_r$. This corresponds to the voltage–current observer block in Fig. 1.

In the actual implementation of (1), a low-pass filter is used instead of a pure integrator. This choice reduces drifts due to errors and offsets in the acquired signals. However, the use of the low-pass filter results in a wrong computation of the rotor flux space vector in terms of magnitude and angle. An estimate of the stator pulsation is used to compensate for these errors, i.e.,

$$\widehat{\omega}_s = \frac{R_rL_m}{L_r}\frac{i_q^*}{\Phi_r^*} + p\omega_r \tag{2}$$

where ω_r is the measured mechanical speed, p is the pole pairs number, i_q^* is the reference value for the torque current, Φ_r^* is the reference value for the rotor flux, and R_r is the rotor resistance.

Relationship (2) is represented in Fig. 1 by the stator frequency estimation block and is used for three main purposes. It is used as the feed-forward compensation in the phase-locked loop (PLL) block used for the tracking of the flux angle. As stated previously, it is used to compensate for errors in the magnitude and the angle of the rotor flux caused by the low-pass filter used for the integration. Eventually, it is used in the decoupling terms that are blocked together with the magnitude of the rotor flux estimated by (1) and the measured currents in the synchronous reference frame to compute the dynamic back-electromotive-force compensation terms

$$\tilde{v}_d = -\widehat{\omega}_s\sigma L_s i_q \tag{3}$$

$$\tilde{v}_q = \widehat{\omega}_s\left(\sigma L_s i_d + \frac{L_m}{L_r}|\overline{\Phi}_r|\right). \tag{4}$$

The magnitude of the estimated flux Φ_r is eventually used as a feedback signal for the outer loop. The output of the PLL block, which is the tracked and corrected rotor flux angle $\tilde{\theta}_s$, is used for the reference frame matrix transformations $P(\tilde{\theta}_s)$ and $P^{-1}(\tilde{\theta}_s)$.

The value of the reference quadrature stator current is obtained from the reference torque and the reference flux signal through the following equation:

$$i_q^* = K_T\frac{T^*}{\Phi_r^*} \tag{5}$$

where $K_T = (2L_r/3pL_m)$. On the other hand, the reference flux is obtained by relying on the nominal values for the torque and the rotor flux, i.e.,

$$\Phi_r^* = \sqrt{\frac{T^*}{T_{\rm nom}}}\Phi_{r_{\rm nom}}. \tag{6}$$

This choice keeps the slip frequency quite constant, providing better robustness of the control system against speed errors and reducing the losses at low torque. This is suited to traction applications, where high-torque dynamics are not requested, and it does not prevent reaching the maximum torque at low speed when needed. In this paper, reference is made to an induction motor drive fed by a pulsewidth modulation (PWM) VSI insulated-gate bipolar transistor inverter.

Typically, in traction drive systems, the switching frequency is very low, making the detection of the faults through the signal injection strategy impossible. Moreover, industries are particularly interested in diagnostic techniques that do not require additional sensors. This paper proposes a simple processing technique that exploits already available control signals for the rotor fault diagnosis.

III. Demodulation of Rotor Fault Signatures in Time-Varying Conditions

Traction drive operations require cyclic torque and speed variations. Under the above conditions, the sideband components, whose amplitude must be monitored for diagnostic purposes, are spread in frequency. It turns out that the direct application of the MCSA to machine stator currents or to control variables is not effective. A simple solution for an efficient diagnosis of electrical faults of induction machines under nonstationary conditions is presented here.

A number of adjacent broken bars produce an amplitude modulation in the rotor current, whose carrier is $s\omega_s$, where s is the slip, $\omega_s = 2\pi f$ is the stator pulsation, and f is the stator frequency. This modulation is reported to the stator quantities at $\omega_l = (1-2s)\omega_s$ and at $\omega_r = (1+2s)\omega_s$ because of the speed ripple effect [24]. Neglecting other effects, like slotting and saturation, it can be assumed that the major components of a stator phase current are represented by

$$i_s(t) = I\cos(\omega_s t + \varphi_s) + I_l\cos(\omega_l t + \varphi_l) + I_r\cos(\omega_r t + \varphi_r). \tag{7}$$

In time-varying conditions, amplitudes I_l and I_r cannot be detected through a frequency analysis since ω_l and ω_r are spread across a wide frequency range, making it impossible to correctly detect their amplitude. In fact, sideband components ω_l and ω_r vary as a function of time according to machine slip and supply frequency.

A simple processing of a phase current can be made, so that all the information related to the fault is reported to a single component, whose amplitude is related to the amplitude of the

left sideband component ω_l and whose pulsation is constant regardless of the machine slip and stator pulsation variations [25].

Specifically, a frequency shift is applied at each time slice so that the left sideband is moved to a far pulsation ω_d, i.e.,

$$i^l_{\rm dem}\left(t,\omega^l_c\right) = i_s(t)e^{\jmath\omega^l_c t} \tag{8}$$

where

$$\omega^l_c(t) = \omega_d - \omega_l(t). \tag{9}$$

To avoid harmonic noise, integral quantities are used, and $\omega_l(t)$ is estimated starting from the rotor electrical angle $\theta_r(t) = (1-s)\omega_s t$ and the stator voltage phase angle $\theta_s(t) = \omega_s t$. Hence, $\omega_l(t)t = 2\theta_r - \theta_s$.

θ_r is obtained by measuring the motor speed with an optical encoder, whereas θ_s is not directly obtained from (2). This angle is $\tilde{\theta}_s$ tracked by the PLL block in Fig. 1. Hence, the computation of the above quantities is intrinsically made by the vector control structure detailed in Section II; thus, the tracking of the carrier ω^l_c is accurate provided that the drive is working correctly.

The sensitivity of the proposed method to motor parameters is quite small. An error in the motor parameters would particularly affect the estimation of the rotor flux (1) in terms of magnitude and angle, and, thus, the decoupling of the axis would not be accurate. However, the closed-loop structure forces the stator frequency of the machine to be equal to the frequency estimated by $\tilde{\theta}_s$; thus, the demodulation based on (9) is correct independently of motor parameter errors.

If the speed sensor failed, the control system would fail; hence, a fault alarm at a higher level would be raised, and a diagnostic procedure would be activated independently. For the purpose of rotor fault detection, it can be assumed with no restrictions that the speed sensor provides accurate information, and that the diagnosis of the whole drive is demanded for a higher level protection system.

Similarly, a stator current may be processed so that the component at ω_r is reported to ω_d, i.e.,

$$i^r_{\rm dem}\left(t,\omega^r_c\right) = i_s(t)e^{\jmath\omega^r_c t} \tag{10}$$

where $\omega^r_c(t) = \omega_d - \omega_r(t)$, and the right sideband pulsation is computed by relying on integral quantities $\omega_r(t)t = 3\theta_s - 2\theta_r$.

A combination of the two demodulated currents can be used to retrieve a diagnostic index that is independent of inertia [6]. If necessary, a similar procedure may be applied to other quantities to avoid the masking effect of drive regulators.

Due to the above-described current demodulation procedure, a diagnostic index can be defined that is quite robust with respect to speed variations and sensitive enough to provide an effective fault detection. Reference is made to the drive structure detailed in Section II. A diagnostic index fi is defined as

$$fi = \frac{\left\langle\left|i^l_{\rm dem}(t,\omega_l)\right|\right\rangle + \left\langle\left|i^r_{\rm dem}(t,\omega_r)\right|\right\rangle}{\left\langle\left|i_q(t)\right|\right\rangle} \tag{11}$$

where $\langle|\times|\rangle$ is the time-domain average of the absolute value of the signal, and $i^l_{\rm dem}(t,\omega_l)$ and $i^r_{\rm dem}(t,\omega_r)$ are computed as in (8) and (10), respectively, with $\omega_d = 0$.

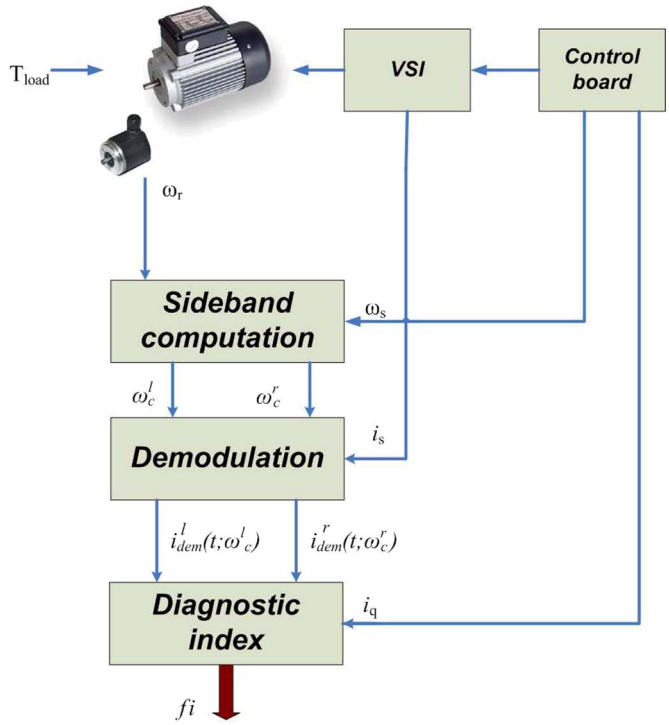

Fig. 2. Block diagram of the proposed diagnostic procedure.

TABLE I
INDUCTION MOTOR PARAMETERS

Parameter	Unit	Value
Rated power	kW	7.5
Rated stator voltage	V	380
Nominal stator current	A	15.3
Rated frequency	Hz	50
Rated speed	rpm	1440
Stator phase resistance	Ω	0.54
Rotor phase resistance	Ω	0.58
Stator inductance	mH	88.4
Rotor inductance	mH	83.3
Magnetizing inductance	mH	81.7
Pole pairs		2
Number of rotor bars		28

Usually, for a mains-supplied machine, the diagnostic indexes are computed with reference to the amplitude of the stator current. In a direct rotor flux field-oriented vector control, the only nonnegligible current in the machine rotor is the torque current under steady-state conditions. In the proposed diagnostic index, the stator torque current $i_q(t)$ was used as a normalization factor since it is proportional to the torque current in the rotor.

A complete diagnostic procedure is possible as detailed in Fig. 2.

IV. SIMULATION RESULTS

Extensive research activities were carried out to model rotor asymmetries to accurately predict the behavior of the machine under faulty conditions [7], [26], [27]. Here, the proposed procedure was validated with a machine model [28], whose parameters are taken from the machine used for the experiments. Specifically, a 7.5-kW three-phase two-pole pairs induction machine was used to verify the agreement between simulations and experiments, and its parameters are shown in Table I.

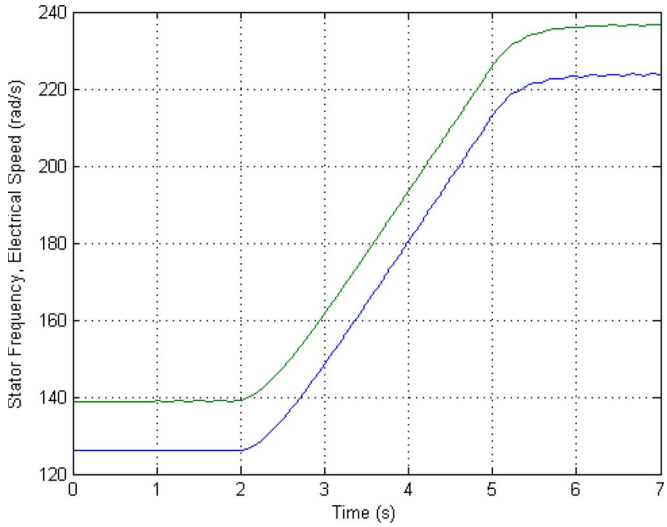

Fig. 3. Simulation results for the 7.5-kW machine. Motor speed transient for the faulty machine. (Top) Stator frequency and (bottom) electrical speed in radians per second.

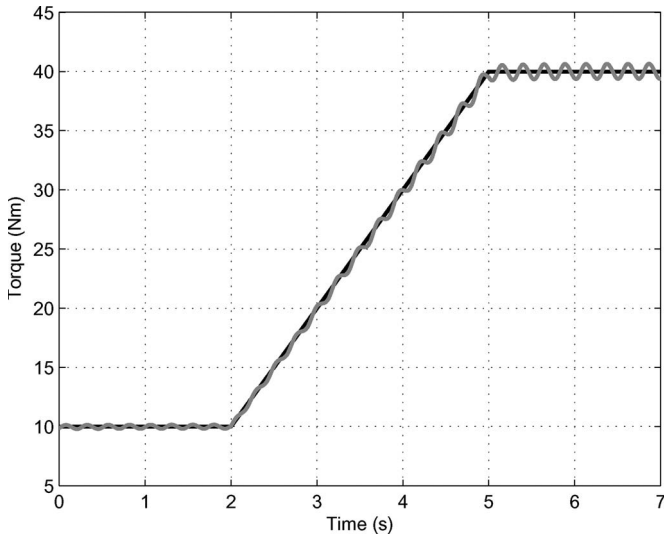

Fig. 4. Simulation results for the 7.5-kW machine. Torque waveforms for the faulty machine. (Solid line) Set point and (light-gray solid line) actual value.

The rotor fault is one broken bar that was modeled increasing the resistance of one squirrel cage rotor bar.

The machine model was used within a dynamic simulation, including the rotor flux field-oriented vector control structure (Fig. 1).

Simulations were made by analyzing an acceleration transient starting with an electrical speed of 125 up to 225 rad/s, with a ramp in the torque command whose duration is about 3 s. This choice was made to comply with the typical torque transient specifications of a railway traction system.

This choice was made to mimic the torque transient of the railway system before the torque limitation. The corresponding stator frequency and motor speed and torque are reported in Figs. 3 and 4, respectively.

Fig. 5 shows the spectrum of a phase current for the 7.5-kW machine in healthy and faulty conditions during the above-described transient.

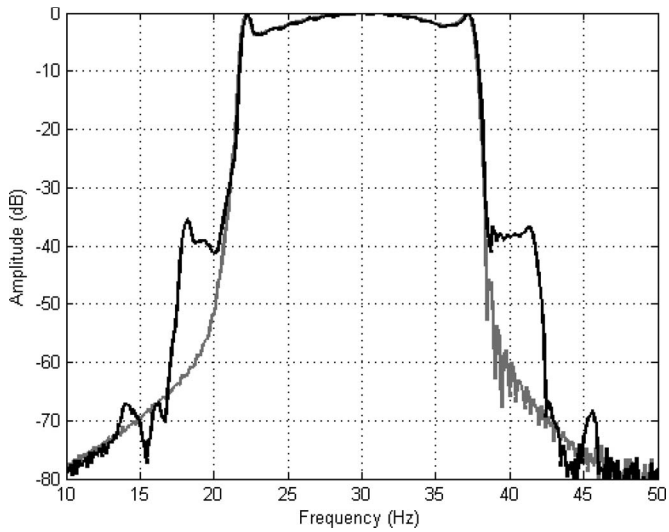

Fig. 5. Simulation results for the 7.5-kW machine. Spectrum of a phase current in (light-gray solid line) healthy and (solid line) faulty conditions.

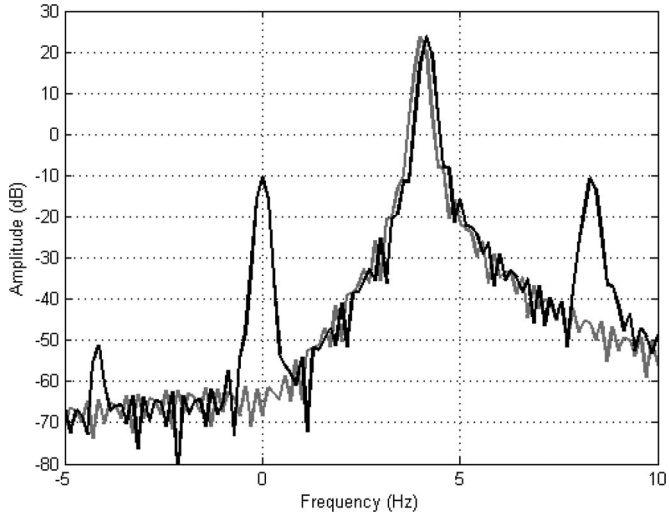

Fig. 6. Simulation results for the 7.5-kW machine. Spectrum of the demodulated current i^l_{dem} in (light-gray solid line) healthy and (solid line) faulty conditions in the range [−5 Hz, 15 Hz] with $\omega_d = 0$.

The spectra show that no signature analysis is possible for such cases because of the large spreading of frequency and speed. Hence, the sideband components related to the faults are spread across a wide frequency range.

Fig. 6 shows the spectrum of a phase current during the same transient after the demodulation process detailed in Section III for the faulty and healthy machine, with $\omega_d = 0$ rad/s. The proposed procedure allows the accurate statement of the amplitude of the sideband components related to the fault.

It is noteworthy to mention that this procedure is perfectly suited to a closed-loop system with low slip variations. In fact, with the adopted closed-loop system, speed and frequency vary accordingly (Fig. 3), so that shifting the left sideband results in reporting to a single line the fundamental and sideband components. On the other hand, in the case of an open-loop control, the fundamental is almost constant, whereas the slip changes remarkably. Hence, the demodulating process would spread the fundamental, making the procedure less effective.

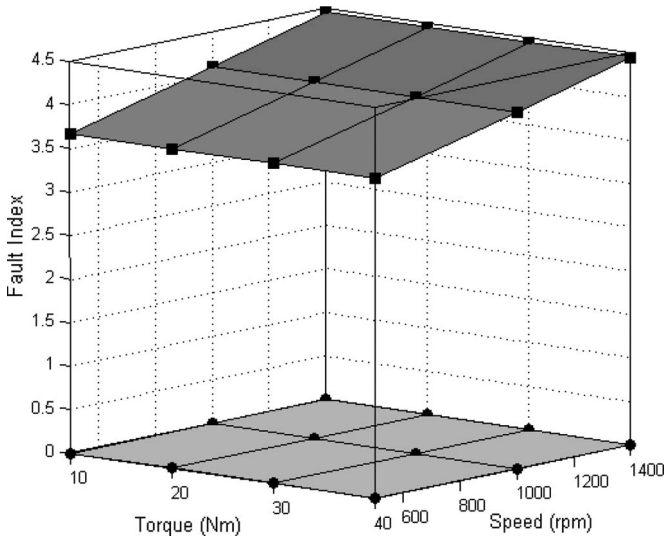

Fig. 7. Simulation results for the 7.5-kW machine. Fault index fi as a function of load torque and speed in (top) faulty and (bottom) healthy conditions.

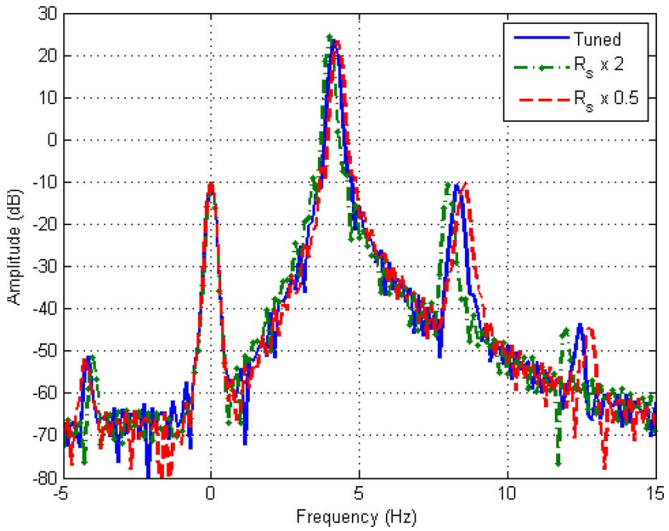

Fig. 8. Simulation results for the 7.5-kW machine. Spectrum of the demodulated current $i^l_{\rm dem}$ for the faulty machine with the actual value of (solid line) R_s, (dashed line) $R_s/2$, and (dash-dotted line) $R_s \times 2$ in the range [−5 Hz, 15 Hz] with $\omega_d = 0$.

The proposed procedure may fail during torque inversions since the slip varies from positive to negative values, causing wide spreading of the fundamental frequency across the spectrum, which can cover the two sideband components.

For the above-described transient, the diagnostic fault index fi computed as in (11) is equal to 3.978 and 0.003 for the faulty and healthy cases, respectively. In Fig. 7, the computation of the same index is reported for different values of load torque and speed in steady-state conditions. This chart confirms that the proposed diagnostic index is quite robust versus load torque and speed variations, whereas the simulations in transient conditions prove that the index is quite sensitive to rotor faults in time-varying conditions.

Eventually, simulations with incorrect motor parameters were made for the faulty machine to confirm the low sensitivity to the parameter variations of the proposed procedure. Figs. 8

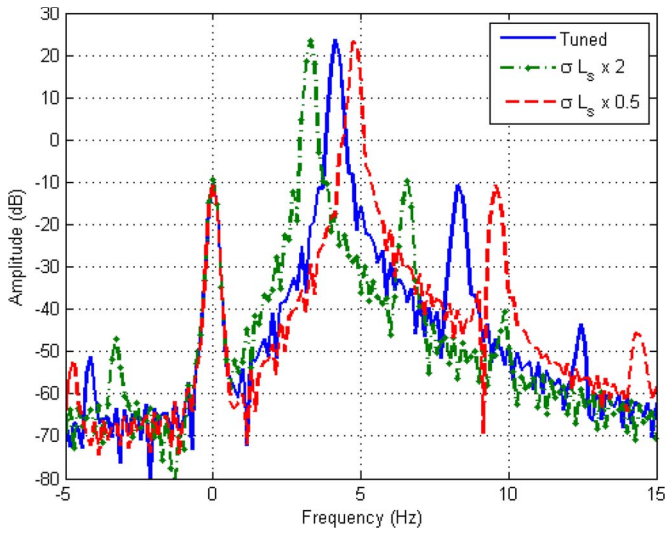

Fig. 9. Simulation results for the 7.5-kW machine. Spectrum of the demodulated current $i^l_{\rm dem}$ for the faulty machine with the actual value of (solid line) σL_s, (dashed line) $\sigma L_s/2$, and (dash-dotted line) $\sigma L_s \times 2$ in the range [−5 Hz, 15 Hz] with $\omega_d = 0$.

Fig. 10. Photos of the (left) test bed and of the (right) drilled rotor bar.

and 9 show that the effect of parameter detuning on the demodulation process is small. The component at zero frequency is almost unaffected by the changes.

Specifically, the stator resistance and the stator transient leakage inductance were modified by a factor of two. These are the most relevant parameters for the rotor flux estimation. Larger errors in the motor parameters would prevent the correct operation of the control system, making it unstable. Hence, for the purpose of rotor fault detection, it can be assumed with no restrictions that this tolerance for the motor parameter is satisfactory.

V. Experimental Results

A thorough set of experiments were performed to validate the proposed method and the effectiveness of the related diagnostic index. To this aim, a test bed was realized (left in Fig. 10) with the machine whose nameplate is reported in Table I. A scaled prototype of the machine and a control system for the traction applications were used.

Two rotors are available: one healthy and the other with one drilled rotor bar (right in Fig. 10). The machine is supplied by

TABLE II
MAIN PARAMETERS OF VECTOR CONTROL REGULATORS

	PI_q	PI_f	PI_d
Proportional gain (k_p)	5	32	5
Integral gain (k_i)	340	230	340

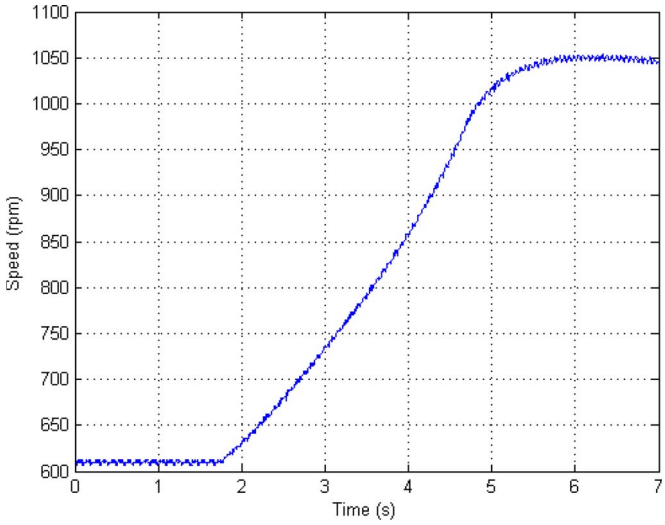

Fig. 11. Experimental results for the 7.5-kW induction machine. Time-domain waveforms of machine speed during acceleration.

a PWM-VSI power converter and is controlled by the direct field-oriented control detailed in Section II and implemented on a dSPACE DS1103 board. The main parameters of the PI regulators are reported in Table II, making reference to the following transfer function for the controllers $\mathrm{PI(s)} = k_p + k_i/\mathrm{s}$. The first column reports the proportional and integral gains for the q-axis current regulator, the second column reports the control parameters for the flux regulator, and the third column reports the control parameters for the d-axis current regulator.

The induction motor is coupled to a 9-kW separately excited dc machine used in regenerating operations and fed by a two-quadrant chopper converter to test variable speed transients. Machine currents and speed are sampled at 8 kHz with a time duration of 7 s. A smaller number of points could be used without affecting the performance of the demodulation procedure.

Specifically, the diagnostic procedure was validated with a reference torque profile obtained through a ramp in the torque command from 20% to 80% of the nominal torque in 3 s. The corresponding speed transient is reported in Fig. 11, and the corresponding direct and quadrature stator currents are reported in Fig. 12. i_d varies with the speed because of the choice of the reference flux (6). The waveforms are fairly similar to the simulation results made under the same conditions (Figs. 3 and 4). During this transient acceleration, the slip frequency slightly varies around 2 Hz.

Fig. 13 reports the waveforms of ω_s, $\omega_c^l(t)$, and $\omega_c^r(t)$ during the above-detailed transient. The currents are sampled by the same control board and are processed according to (8), (10), and (11).

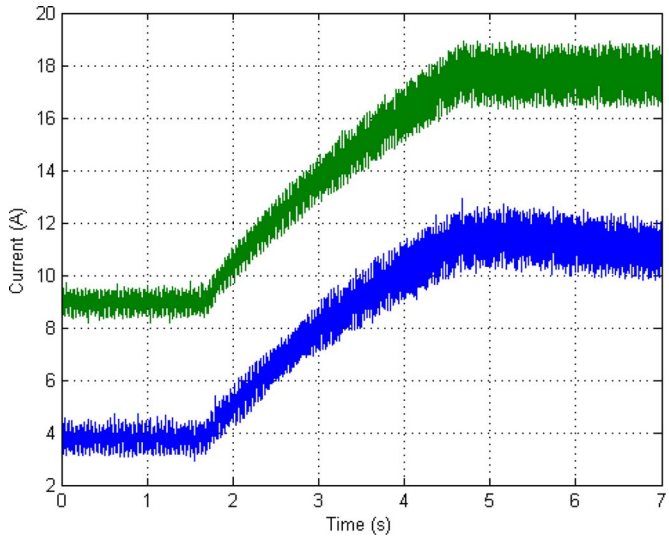

Fig. 12. Experimental results for the 7.5-kW induction machine. Time-domain waveforms of machine currents during acceleration. (Top) i_q and (bottom) i_d.

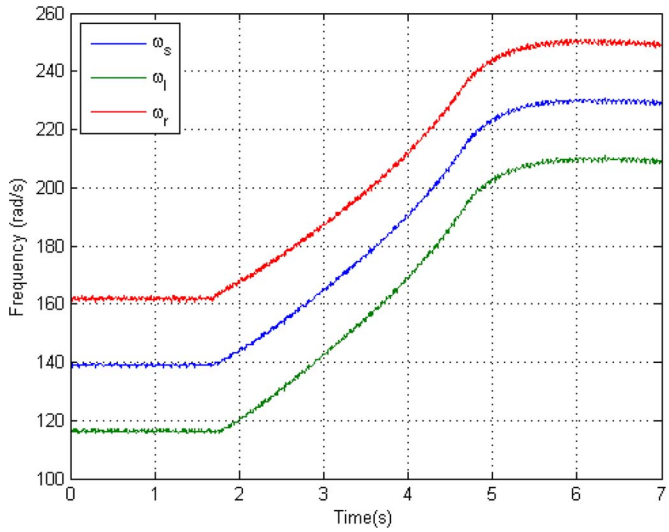

Fig. 13. Experimental results for the 7.5-kW induction machine. Time-domain waveforms of ω_s, $\omega_c^l(t)$, and $\omega_c^r(t)$ during the acceleration transient.

Fig. 14 reports the spectra of a phase current in healthy and faulty conditions during the same machine acceleration.

The spectra show that no signature analysis is possible for such cases because of the large spreading of frequency and speed. Hence, the sideband components related to the faults are spread across a wide frequency range and are not detectable.

Fig. 15 shows the spectrum of the demodulated current during machine acceleration after the demodulation process detailed in Section III for the healthy and faulty machine with $\omega_d = 0$ rad/s.

The proposed procedure allows the accurate statement of the amplitude of the sideband components related to the fault. In fact, the dc component $(\omega_d = 0)$ increases by about 16 dB from healthy to faulty conditions, as shown in Fig. 15. This result is in good agreement with the simulation results under the same conditions (Fig. 6). Anyway, in the experiments, a higher value of the fault signature appears in the healthy case because of

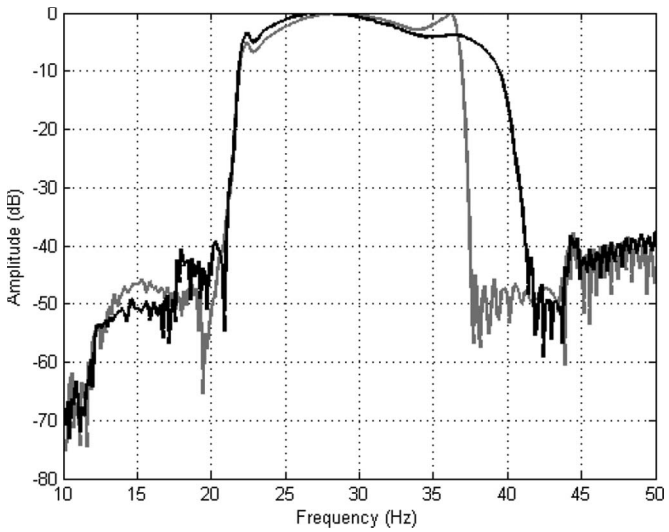

Fig. 14. Experimental results for the 7.5-kW induction machine. Spectrum of a phase current in (light-gray solid line) healthy and (solid line) faulty conditions during acceleration.

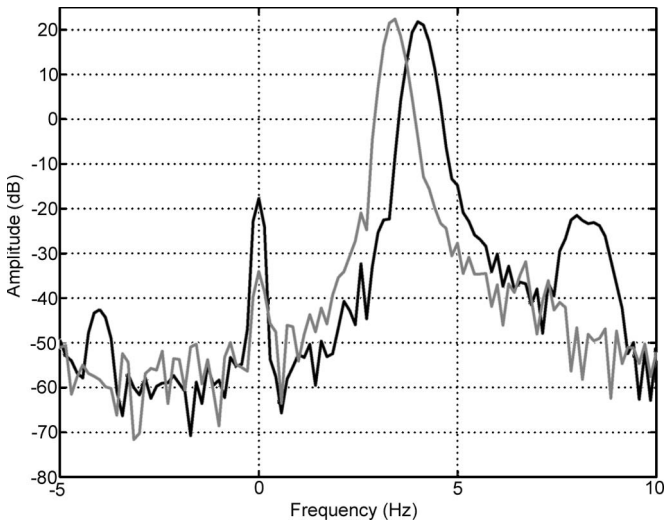

Fig. 15. Experimental results for the 7.5-kW induction machine. Spectrum of the demodulated current $i^l_{\rm dem}$ for the machine in (light-gray solid line) healthy and (solid line) faulty conditions during acceleration with $\omega_d = 0$.

intrinsic manufacturing rotor asymmetry, whereas a lower value of the fault signature appears in the faulty case since magnetic saturation and interbar currents are not included in the machine model.

Then, the diagnostic index fi is computed as in (11). During the above-detailed acceleration transient, fi is equal to 0.269 and 1.735 for the healthy and faulty cases, respectively, proving its sensitivity to rotor faults in time-varying conditions.

Fig. 16 reports the values of the fault index in steady-state conditions for different load torque and speeds. It turns out that the fault index is quite robust against speed variations, but slightly dependent on load torque variations. In fact, the flux level in the machine accordingly changes to the square root of the torque; thus, the absolute value of the index changes because of the nonlinear nature of the induction motor. This behavior prevents a quantitative analysis of the fault severity,

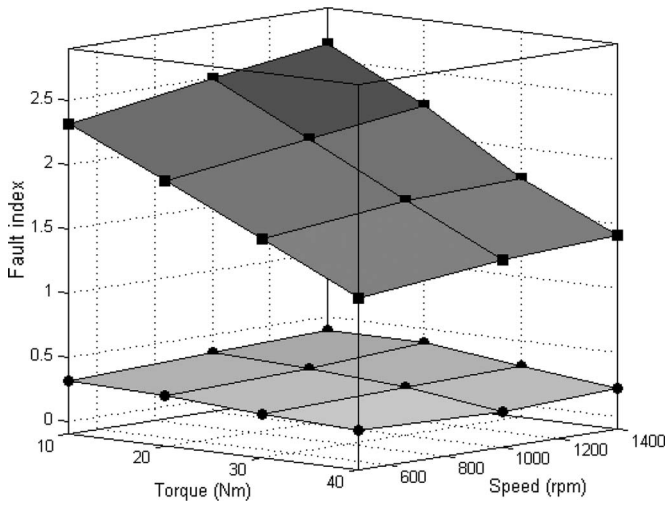

Fig. 16. Experimental results for the 7.5-kW induction machine. Fault index fi as a function of load torque and speed at (top) faulty and (bottom) healthy conditions.

whereas the fault detection capability is still very good in any conditions, as reported in Fig. 16.

VI. Conclusion

A diagnostic procedure for rotor faults of induction machine drives in time-varying conditions has been proposed here.

The method has been tailored to direct rotor flux field-oriented controlled drives in transient conditions. During transient operations, torque and speed vary, preventing the use of the MCSA and traditional spectral analysis for an effective diagnosis of rotor faults.

Due to the proposed approach, the currents have been demodulated to report to the single-frequency time-varying components related to rotor faults. Compared with the solutions that use time–frequency distributions, the proposed procedure requires simpler processing; moreover, it exploits the observers of the drive control to achieve optimal demodulation results.

A diagnostic index has been proposed that is quite robust versus load and inertia variations and sensitive enough to provide effective fault detection. Simulation and experimental results referred to typical specifications of variable speed drives for traction applications have been reported that confirm the validity of the proposed method.

References

[1] P. H. Mellor, T. J. Allen, R. Ong, and Z. Rahma, "Faulted behaviour of permanent magnet electric vehicle traction drives," in *Proc. IEEE IEMDC*, Jun. 2003, vol. 1, pp. 554–558.

[2] M. W. Winterling, E. Tuinman, and W. Deleroi, "Fault analysis of electro-mechanical traction drives," in *Proc. 8th Int. Conf. Elect. Mach. Drives (Conf. Publ. No. 444)*, Cambridge, U.K., Sep. 1997, pp. 248–252.

[3] C. Kral, F. Pirker, and G. Pascoli, "Detection of rotor faults in inverter fed induction machines by means of the Vienna monitoring method—A proposed application for traction drives," in *Proc. 1st Int. Conf. Railway Traction Syst., RTS 3*, Capri, Italy, May 2001, pp. 79–89.

[4] A. H. Bonnett and C. Yung, "Increased efficiency versus increased reliability," *IEEE Ind. Appl. Mag.*, vol. 14, no. 1, pp. 29–36, Jan./Feb. 2008.

[5] M. El Hachemi Benbouzid, "A review of induction motors signature analysis as a medium for faults detection," *IEEE Trans. Ind. Electron.*, vol. 47, no. 5, pp. 984–993, Oct. 2000.

[6] A. Bellini, F. Filippetti, G. Franceschini, C. Tassoni, and G. B. Kliman, "Quantitative evaluation of induction motor broken bars by means of electrical signature analysis," *IEEE Trans. Ind. Appl.*, vol. 37, no. 5, pp. 1248–1255, Sep./Oct. 2001.
[7] H. Henao, H. Razik, and G. A. Capolino, "Analytical approach of the stator current frequency harmonics computation for detection of induction machine rotor faults," *IEEE Trans. Ind. Appl.*, vol. 41, no. 3, pp. 801–807, May/Jun. 2005.
[8] J. H. Jung, J. J. Lee, and B. H. Kwon, "Online diagnosis of induction motors using MCSA," *IEEE Trans. Ind. Electron.*, vol. 53, no. 6, pp. 1842–1852, Dec. 2006.
[9] R. R. Schoen and T. G. Habetler, "Effects of time-varying loads on rotor fault detection in induction machines," *IEEE Trans. Ind. Appl.*, vol. 31, no. 4, pp. 900–906, Jul./Aug. 1995.
[10] R. S. Wieser, C. Kral, and F. Pirker, "The Vienna induction machine monitoring method; on the impact of the field oriented control structure on real operational behavior of a faulty machine," in *Proc. 24th Annu. Conf. IEEE IECON*, Aachen, Germany, Aug./Sep. 1998, vol. 3, pp. 1544–1549.
[11] A. Bellini, F. Filippetti, G. Franceschini, and C. Tassoni, "Closed-loop control impact on the diagnosis of induction motors faults," *IEEE Trans. Ind. Appl.*, vol. 36, no. 5, pp. 1318–1329, Sep./Oct. 2000.
[12] D. Casadei, F. Filippetti, C. Rossi, A. Stefani, A. Yazidi, and G. A. Capolino, "Diagnostic technique based on rotor modulating signals signature analysis for doubly fed induction machines in wind generator systems," in *Conf. Rec. 41st IEEE IAS Annu. Meeting*, Tampa, FL, Oct. 2006, vol. 3, pp. 1525–1532.
[13] I. Jaksch, "Faults diagnosis of three-phase induction motors using envelope analysis," in *Proc. 4th IEEE Int. SDEMPED*, Aug. 2003, pp. 289–293.
[14] C. Kral, R. S. Wieser, F. Pirker, and M. Schagginger, "Sequences of field-oriented control for the detection of faulty rotor bars in induction machines—The Vienna monitoring method," *IEEE Trans. Ind. Electron.*, vol. 47, no. 5, pp. 1042–1050, Oct. 2000.
[15] F. Briz, M. W. Degner, A. B. Diez, and J. M. Guerrero, "Online diagnostics in inverter-fed induction machines using high-frequency signal injection," *IEEE Trans. Ind. Appl.*, vol. 40, no. 4, pp. 1153–1161, Jul./Aug. 2004.
[16] S. H. Kia, H. Henao, and G. A. Capolino, "A high-resolution frequency estimation method for three-phase induction machine fault detection," *IEEE Trans. Ind. Electron.*, vol. 54, no. 4, pp. 2305–2314, Aug. 2007.
[17] S. Rajagopalan, J. M. Aller, J. A. Restrepo, T. G. Habetler, and R. G. Harley, "Detection of rotor faults in brushless dc motors operating under nonstationary conditions," *IEEE Trans. Ind. Appl.*, vol. 42, no. 6, pp. 1464–1477, Nov./Dec. 2006.
[18] M. Blodt, D. Bonacci, J. Regnier, M. Chabert, and J. Faucher, "On-line monitoring of mechanical faults in variable-speed induction motor drives using the Wigner distribution," *IEEE Trans. Ind. Electron.*, vol. 55, no. 2, pp. 522–533, Feb. 2008.
[19] L. Eren and M. J. Devaney, "Motor bearing damage detection via wavelet analysis of the starting current transient," in *Proc. 18th IEEE IMTC*, Budapest, Hungary, 2001, vol. 3, pp. 1797–1800.
[20] H. Douglas, P. Pillay, and A. K. Ziarani, "A new algorithm for transient motor current signature analysis using wavelets," *IEEE Trans. Ind. Appl.*, vol. 40, no. 5, pp. 1361–1368, Sep./Oct. 2004.
[21] H. Douglas, P. Pillay, and A. K. Ziarani, "Broken rotor bar detection in induction machines with transient operating speeds," *IEEE Trans. Energy Convers.*, vol. 20, no. 1, pp. 135–141, Mar. 2005.
[22] J. Cusido, L. Romeral, J. A. Ortega, J. A. Rosero, and A. Garcia Espinosa, "Fault detection in induction machines using power spectral density in wavelet decomposition," *IEEE Trans. Ind. Electron.*, vol. 55, no. 2, pp. 633–643, Feb. 2008.
[23] J. Holtz, "Sensorless control of induction motor drives," *Proc. IEEE*, vol. 90, no. 8, pp. 1359–1394, Aug. 2002.
[24] F. Filippetti, G. Franceschini, C. Tassoni, and P. Vas, "AI techniques in induction machines diagnosis including the speed ripple effect," *IEEE Trans. Ind. Appl.*, vol. 34, no. 1, pp. 98–108, Jan./Feb. 1998.
[25] A. Stefani, F. Filippetti, and A. Bellini, "Diagnosis of induction machines in time-varying conditions," in *Proc. IEEE Int. SDEMPED*, Cracow, Poland, Sep. 2007, pp. 126–131.
[26] H. Henao, C. Martis, and G. A. Capolino, "An equivalent internal circuit of the induction machine for advanced spectral analysis," *IEEE Trans. Ind. Appl.*, vol. 40, no. 3, pp. 726–734, May/Jun. 2004.
[27] X. Tu, L. A. Dessaint, M. El Kahel, and A. O. Barry, "A new model of synchronous machine internal faults based on winding distribution," *IEEE Trans. Ind. Electron.*, vol. 53, no. 6, pp. 1818–1828, Dec. 2006.
[28] P. Vas, F. Filippetti, G. Franceschini, and C. Tassoni, "Transient modelling oriented to diagnostics of induction machines with rotor asymmetries," in *Proc. ICEM*, Paris, France, 1994, pp. 60–66.

Andrea Stefani was born in Bologna, Italy, in 1976. He received the M.S. degree (with honors) in electrical engineering in 2004 from the University of Bologna, Bologna, where he is currently working toward the Ph.D. degree in the Department of Electrical Engineering.

Since 2005, he has been a Research Collaborator with the Department of Electrical Engineering, University of Bologna. His research interests are related to electrical machines and drives, diagnostics of induction motors, and renewable energy. His current activities include control and diagnosis of induction machines in wind generator and railway traction systems.

Alberto Bellini (S'96–M'99) was born in Italy in 1969. He received the Laurea degree (M.S.) in electronic engineering and the Ph.D. degree in computer science and electronic engineering from the University of Bologna, Bologna, Italy, in 1994 and 1998, respectively.

From 1999 to 2004, he was with the University of Parma, Parma, Italy. In 2000, he was an Honorary Scholar with the University of Wisconsin, Madison. Since 2004, he has been with the University of Modena and Reggio Emilia, Reggio Emilia, Italy, where he is currently an Assistant Professor in electric machines and drives. He has authored or coauthored more than 80 papers and one textbook. He is the holder of three industrial patents. His research interests include power electronics, signal processing for audio and industrial applications, and electric drive design and diagnosis.

Dr. Bellini was the recipient of the 2001 First Prize Paper Award from the Electric Machines Committee of the IEEE Industry Applications Society. He is a member of the Italian Association of Converters, Electrical Machines and Drives. He has served as an Associate Editor of the IEEE TRANSACTIONS ON INDUSTRIAL ELECTRONICS.

Fiorenzo Filippetti (M'00) was born in Fano, Italy, in 1945. He received the M.S. degree in electrical engineering from the University of Bologna, Bologna, Italy, in 1970.

In 1976, he was an Assistant Professor with the Department of Electrical Engineering, University of Bologna, where he is currently a Full Professor in electrical drives. From 1993 to 2002, he was an Adjoint Professor in electrotechnics and electrical drives with the University of Parma, Parma, Italy. In 1998, he was a member with the Scientific Council, Centre de Génie Electrique de Lyon (CEGELY), University Claude Bernard, Lyon, France. He spent several visiting periods with CEGELY and with the University of Picardie Jules Verne, Amiens, France. In 2004, he was a Lecturer for the European Master in Advanced Power Electrical Engineering recognized by the European Commission. He has been the Advisor of various Ph.D. and M.S. students. He is involved in national and European research projects. He has authored or coauthored one textbook and more than 160 scientific papers published in scientific journals and conference proceedings since 1976. He is the holder of an industrial patent. His main research interests include the simulation and modeling of electric circuits and systems, and the study and application of condition monitoring and fault detection techniques for ac electrical machinery.

Prof. Filippetti is a member of the steering committees of various international conferences. He was the recipient of the Oral Presentation Best Paper Award at the 2000 IEEE Industry Applications Conference, Rome, Italy. He is a Registered Professional Engineer in the Province of Bologna, a member of the Italian Association of Electrical and Electronics Engineers, and a member of the Italian Association of Converters, Electrical Machines and Drives.